ACS APPLIED MATERIALS & INTERFACES

Research Article

www.acsami.org

Functionalized Porous Aromatic Framework for Efficient Uranium Adsorption from Aqueous Solutions

Baiyan Li,[†] Qi Sun,[†] Yiming Zhang,[†] Carter W. Abney,[‡,§] Briana Aguila,[†] Wenbin Lin,[‡] and Shengqian Ma*[,†]

[†]Department of Chemistry, University of South Florida, 4202 E. Fowler Avenue, Tampa, Florida 33620, United States

[‡]Department of Chemistry, University of Chicago, 929 East 57th St., Chicago, Illinois 60637, United States

[§]Chemical Sciences Division, Oak Ridge National Laboratory, P.O. Box 2008, Oak Ridge, Tennessee 37831, United States

Supporting Information

ABSTRACT: We demonstrate the successful functionalization of a porous aromatic framework for uranium extraction from water as exemplified by grafting PAF-1 with the uranyl chelating amidoxime group. The resultant amidoxime-functionalized PAF-1 (PAF-1-CH_2AO) exhibits a high uranium uptake capacity of over 300 mg g^{-1} and effectively reduces the uranyl concentration from 4.1 ppm to less than 1.0 ppb in aqueous solutions within 90 min, well below the acceptable limit of 30 ppb set by the US Environmental Protection Agency. The local coordination environment of uranium in PAF-1-CH_2AO is revealed by X-ray absorption fine structure spectroscopic studies, which suggest the cooperative binding between UO_2^{2+} and adjacent amidoxime species.

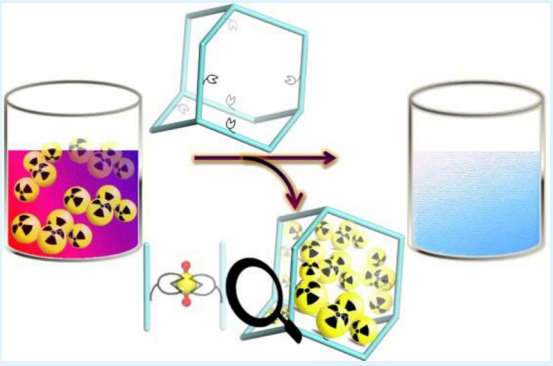

KEYWORDS: *porous aromatic framework, uranium adsorption, amidoxime chelating group, postsynthetic modification, radionuclide migration*

INTRODUCTION

The development of technologies for efficient extraction of uranium from aqueous solutions has long been of great interest.[1−3] This is primarily prompted by two incentives: one is the energy perspective, given uranium is the main fuel for nuclear energy with its largest source in seawater but at extremely low concentrations (3−3.3 ppb);[4] the other is the environmental perspective, since uranium is the dominant component of nuclear waste and has hazardous effects on the environment, ecosystem, and human health.[5] Various adsorbent technologies based upon synthetic organic polymers,[6−11] biopolymers,[12,13] inorganic materials,[14−18] mesoporous silica materials,[19,20] porous carbon-based adsorbents,[21,22] ionic liquids,[23] and metal−organic frameworks (MOFs)[24−26] have been explored for uranium adsorption. However, these benchmark sorbent materials suffer from a number of drawbacks such as low adsorption capacity, slow kinetics, weak binding affinity, and poor water/chemical stability. Hence, there is still a need to develop new adsorbent materials for efficient uranium extraction from aqueous solutions.

Emerging as a new class of adsorbent materials, porous organic polymers (POPs)[27−29] have recently attracted increasing interest because of their high surface areas, tunable pore sizes, and with the ability to incorporate specific functionality. POPs thus have great potential for various applications, such as gas storage/separation,[30−32] CO_2 capture,[33,34] hydrocarbon adsorption,[35] catalysis,[36−41] environmental remediation,[42,43] and more.[44,45] Compared with other types of porous materials,[46−51] POPs feature robust covalent framework structures with high water and chemical stability, making them practically useful under harsh conditions. Additionally, their pore walls can be decorated with functional organic groups to selectively capture targeted guest species,[52] offering an opportunity for the development of new types of adsorbent materials for uranium extraction from water. In this contribution, we demonstrate the successful decoration of a POP with uranyl chelating groups; the resultant functionalized POP exhibits a high uranium uptake capacity of over 300 mg g^{-1} and can effectively reduce the uranyl concentration from 4.1 ppm to less than 1.0 ppb in aqueous solutions within 90 min, well below the acceptable limit of 30 ppb defined by the US Environmental Protection Agency (EPA).

EXPERIMENTAL SECTION

Materials. All reagents were purchased from Sigma-Aldrich or Alfa and used as received unless otherwise indicated. PAF-1[53,54] was synthesized according to previously reported procedures.

Adsorbent Synthesis. *Synthesis of PAF-1-CH_2Cl.* A resealable flask was charged with PAF-1 (200.0 mg), paraformaldehyde (1.0 g), glacial AcOH (6.0 mL), H_3PO_4 (3.0 mL) and concentrated HCl (20.0

Received: February 5, 2017
Accepted: March 28, 2017
Published: March 28, 2017

DOI: 10.1021/acsami.7b01711
ACS Appl. Mater. Interfaces 2017, 9, 12511−12517

Scheme 1. Schematic Illustration of the Procedures for the Preparation of PAF-1-CH_2AO: (a) AcOH, H_3PO_4, HCl; (b) NaCN; (c) NH_2·OH

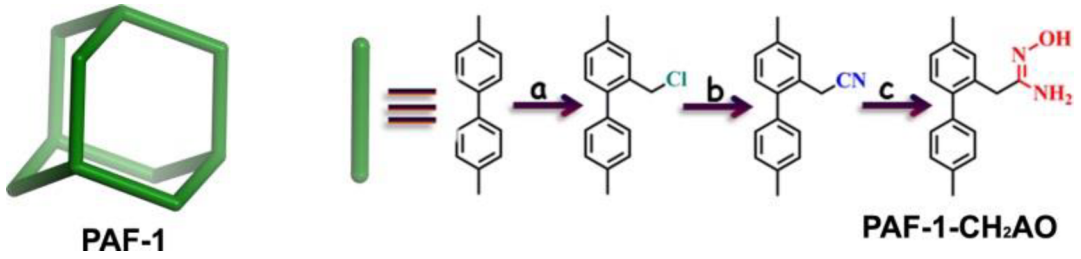

mL). The flask was sealed and heated to 90 °C for 3 days. The resulting solid was filtered, washed with water and methanol, and then dried under vacuum to yield a yellow solid denoted as PAF-1-CH_2Cl.

Synthesis of PAF-1-CH_2CN. The cyano-functionalized PAF-1 was synthesized by treating PAF-1-CH_2Cl (200 mg) with NaCN in 30 mL of EtOH at 80 °C for 3 days under N_2. After being cooled down, the resulting solid was filtered, washed with water and methanol, and then dried under vacuum to yield a light yellow solid denoted as PAF-1-CH_2CN.

Synthesis of PAF-1-CH_2AO. The amidoxime-functionalized PAF-1 (PAF-1-CH_2AO) was synthesized by treating PAF-1-CH_2CN (200 mg) with NH_2OH aqueous solution (50 wt %, 10 mL) and K_2CO_3 (100 mg) in ethanol (20 mL) at 70 °C for 48 h to convert the cyano groups into amidoxime. After being cooled down, the PAF-1-CH_2AO, as an off-white solid, was obtained by filtration, washing with water, and drying under vacuum. The sorbent was treated with 3% (w/w) aqueous potassium hydroxide solution at room temperature for 36 h before uranium adsorption measurements.

Sorption Tests. *Sorption Isotherm Tests.* Samples of 20 mL water were prepared with UO_2^{2+} concentrations in the range 8.6−165.7 ppm at pH ∼ 6. 5 mg of PAF-1-CH_2AO was added to each sample and with continuous stirring at RT overnight. The treated solutions were filtrated through a 0.45 μm membrane filter. The supernatant was analyzed using ICP-OES to determine the remaining UO_2^{2+} concentration. A sample of UO_2^{2+} solution without sorbent material was analyzed during each sorption experiment as a negative control. The sorption capacity q_e (mg g^{-1}) of UO_2^{2+} was calculated with the following equation:

$$q_e = \frac{(C_0 - C_e)V}{m}$$

where C_0 and C_e are the concentration of UO_2^{2+} initially and at equilibrium, respectively. V is the volume of solution, and m is the mass of sorbent used.

UO_2^{2+} Sorption Kinetic Tests. UO_2^{2+} aqueous solution (300 mL, 7.36 ppm, pH ∼ 6) and PAF-1-CH_2AO (3 mg) were added to an Erlenmeyer flask with a magnetic stir bar. The mixture was then stirred at room temperature. At appropriate time intervals, aliquots (5 mL) were taken from the mixture, and the adsorbents were separated by syringe filter (0.45 μm membrane filter). The UO_2^{2+} concentration for 0, 10, 20, 30, 60, 90, and 120 min in the resulting solutions were analyzed by ICP-OES. The sorption capacity q_t (mg g^{-1}) of UO_2^{2+} was calculated with the following equation:

$$q_t = \frac{(C_0 - C_t)V}{m}$$

UO_2^{2+} Removal Efficiency Tests. UO_2^{2+} aqueous solution (200 mL, 4100 ppb, pH ∼ 6) and PAF-1-CH_2AO (10 mg) were added to an Erlenmeyer flask with a magnetic stir bar. The mixture was then stirred at room temperature. At appropriate time intervals, aliquots (3 mL) were taken from the mixture, and the adsorbents were separated by syringe filter (0.45 μm membrane filter). The UO_2^{2+} concentration in the resulting solutions were analyzed by ICP-MS. The percentage removal of UO_2^{2+} was calculated as follows:

$$\text{removal percentage } (\%) = \frac{C_0 - C_t}{C_0} \times 100$$

where C_0 is the initial concentration of UO_2^{2+} and C_t is the UO_2^{2+} concentration at different times.

Simulated Seawater Uranium Adsorption Test. Simulated seawater was prepared as follows: sodium chloride (25.6 g, 438 mmol), sodium bicarbonate (0.193 g, 2.3 mmol), and uranium nitrate hexahydrate were dissolved in distilled water (1.0 L). UO_2^{2+} simulated seawater solution (200 mL, 7.05 ppm) and PAF-1-CH_2AO (5 mg) were added to an Erlenmeyer flask with a magnetic stir bar. The mixture was then stirred at room temperature. At appropriate time intervals, aliquots (5 mL) were taken from the mixture, and the adsorbents were separated by syringe filter (0.45 μm membrane filter). The UO_2^{2+} concentration in the resulting solutions were analyzed by ICP-OES.

Recyclability Test. After one run of adsorption, PAF-1-CH_2AO was regenerated by treatment with Na_2CO_3 (1 M) solution and washed with water. After being dried under vacuum, the resultant material was used for another adsorption experiment. It was found that after two consecutive cycles PAF-1-CH_2AO still showed excellent uranium uptake. The testing conditions are listed as follows: UO_2^{2+} aqueous solution (300 mL, ∼7.5 ppm) and PAF-1-CH_2AO (3 mg) were added to an Erlenmeyer flask with a magnetic stir bar. The mixture was then stirred at room temperature. After 12 h, aliquots (5 mL) were taken from the mixture, and the adsorbents were separated by syringe filter (0.45 μm membrane filter). The UO_2^{2+} concentration in the resulting solution was analyzed by ICP-OES. A sample of UO_2^{2+} solution without sorbent material was analyzed during each sorption experiment as a negative control.

RESULTS AND DISCUSSION

PAF-1 (cross-linked polytetraphenylmethane), which is also known as PPN-6, was selected for our proof-of-principle experiment due to its high surface area and exceptional stability in water/moisture and acidic/basic media.[53,54] Given its excellent chelating ability with uranyl ions, the amidoxime group was chosen to functionalize PAF-1. The amidoxime functionalized PAF-1 (PAF-1-CH_2AO) was synthesized by chloromethylation of PAF-1 followed by treatment with NaCN (PAF-1-CH_2CN) and then amidoximation using hydroxylamine (Scheme 1).[55] The successful grafting of the amidoxime group onto PAF-1 was confirmed by elemental analysis, Fourier transform infrared spectroscopy (FT-IR), and solid-state ^{13}C NMR. Elemental analysis reveals a nitrogen content of 2.38 wt % of PAF-1-CH_2CN corresponding to 1.7 mmol g^{-1} CN groups in PAF-1-CH_2CN. In addition, the FT-IR spectrum of PAF-1-CH_2CN shows the characteristic band of the cyano group at around 2251 cm^{-1}, indicating the introduction of cyano groups on the PAF-1. After amidoximation, the disappearance of the CN peak at 2251 cm^{-1} together with the appearance of C═N (1638 cm^{-1}), C−N (1381 cm^{-1}), and N−O (933 cm^{-1}) in PAF-1-CH_2AO verifies the successful

DOI: 10.1021/acsami.7b01711
ACS Appl. Mater. Interfaces 2017, 9, 12511−12517

transformation of cyano groups to amidoxime groups (Figure 1a). Furthermore, the emergence of peaks at 33.0 and 153.8

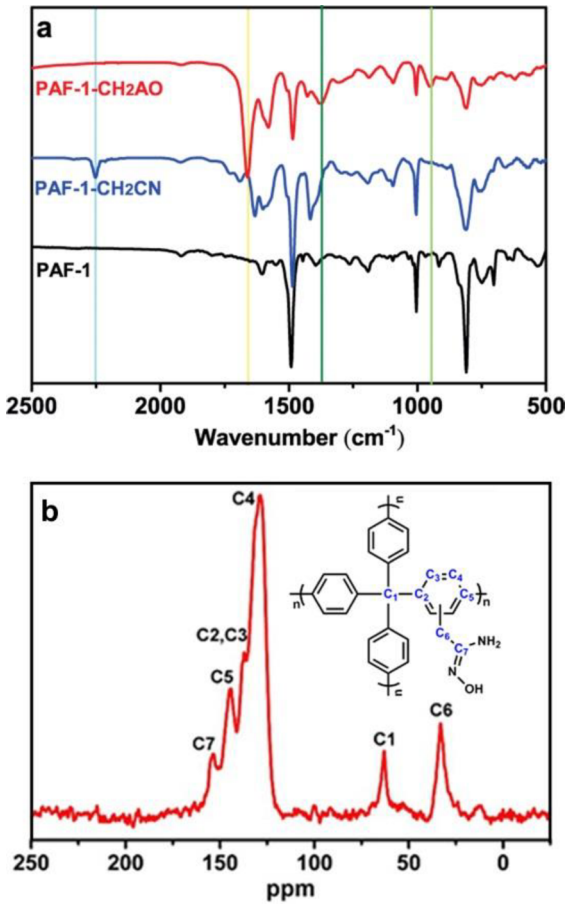

Figure 1. (a) IR spectra of PAF-1, PAF-1-CH_2CN, and PAF-1-CH_2AO. (b) Solid-state ^{13}C NMR spectrum of PAF-1-CH_2AO. N_2 sorption isotherms of PAF-1 (black) and PAF-1-CH_2AO (red).

ppm can be assigned to the carbon of the $-CH_2$ group and amidoxime group, respectively, in the solid-state ^{13}C NMR spectrum of PAF-1-CH_2AO (Figure 1b) and confirms the attachment of $-CH_2AO$ groups to PAF-1. To test the porosity of the materials, nitrogen sorption isotherms were collected at 77 K. As a result of the presence of amidoxime groups in the pores, the Brunauer–Emmett–Teller (BET) surface area is reduced to 855 $m^2\ g^{-1}$ from 4715 $m^2\ g^{-1}$ upon postsynthetic modification (Figure 2). The decreased surface area may be due to the increased mass and pore filling after the functionality addition. Correspondingly, pore size distributions show a clear shrinkage, with pore size maxima shrinking from 14 Å in PAF-1 to 7 Å in PAF-1-CH_2AO (Figure S1).

After confirming the grafting of amidoxime groups and permanent porosity of PAF-1-CH_2AO, we examined its ability to capture uranyl (UO_2^{2+}), the prevalent form of uranium in aqueous solutions. To assess the overall capacity, an adsorption isotherm (Figure 3a) was collected by equilibrating the PAF-1-CH_2AO with a wide range of uranyl concentrations from 8.6 to 165.7 ppm at a phase ratio of 0.25 mg mL^{-1}. The resulting isotherm was well fitted with the Langmuir model, giving rise to a correlation coefficient R^2 = 0.97. The maximum uranium uptake capacity was estimated to be 304 mg g^{-1}, which is among the highest reported values for uranium adsorbent materials.[4−10] Time-course adsorption measurements indicated

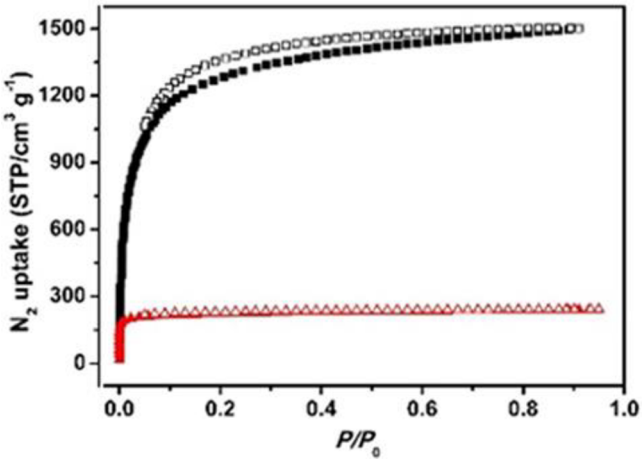

Figure 2. N_2 sorption isotherms of PAF-1 (black) and PAF-1-CH_2AO (red).

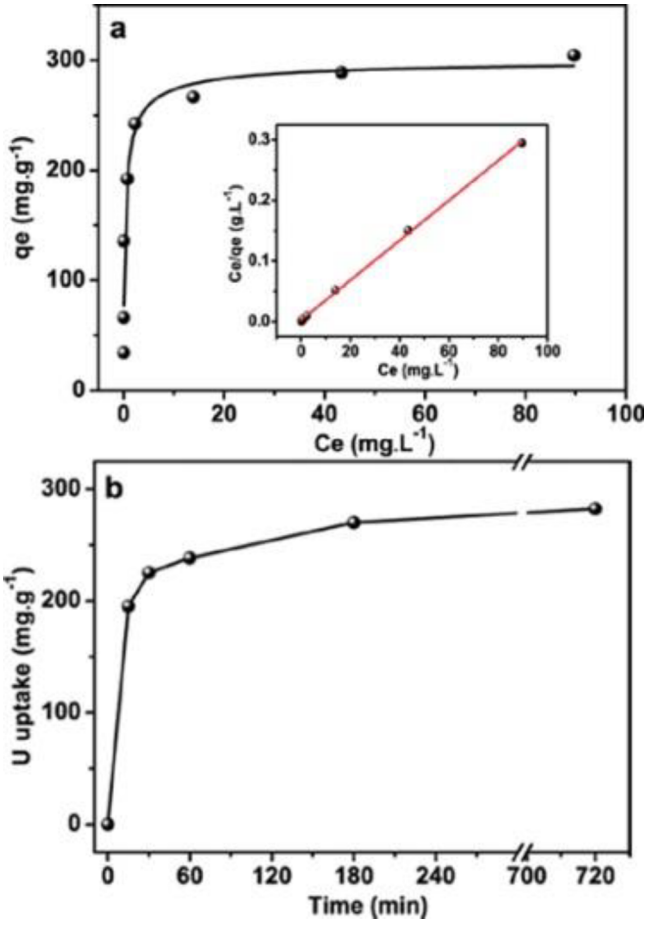

Figure 3. (a) UO_2^{2+} adsorption isotherm for PAF-1-CH_2AO. Inset shows the linear regression by fitting the equilibrium adsorption data with Langmuir adsorption model. (b) Adsorption kinetics of UO_2^{2+} versus contact time in aqueous solution using PAF-1-CH_2AO.

that uranyl capture by PAF-1-CH_2AO is kinetically efficient (Figure 3b), as evidenced by reaching its 84.4% saturation capacity within 1 h with an increase to 95.8% after 3 h. After 12 h, PAF-1-CH_2AO gave rise to an adsorption capacity as high as 283 mg g^{-1}. More significantly, PAF-1-CH_2AO can readily be regenerated by treating it with Na_2CO_3 (1 M), and it was demonstrated to retain its uranium uptake capacity for at least

DOI: 10.1021/acsami.7b01711
ACS Appl. Mater. Interfaces 2017, 9, 12511−12517

two consecutive cycles, affording a value of 271 mg g^{-1}, which is comparable to that of the fresh PAF-1-CH_2AO. While under similar conditions, PAF-1 gave a negligible adsorption amount (less than 10 mg g^{-1}), suggesting that almost all of the captured uranium species are contributed to the grafted amidoxime groups.

Economical and proliferation-resistant management of radioactive waste is a topic of high priority for national security and sustainable power generation. Accordingly, we investigated the effectiveness of PAF-1-CH_2AO for removing UO_2^{2+} from aqueous solutions (Figure 4). In brief, 10 mg of PAF-1-CH_2AO was added to 200 mL of aqueous solution containing 4100 ppb UO_2^{2+}. The concentration of UO_2^{2+} drastically decreased to 12.4 ppb after 60 min of treatment, indicating a removal efficiency of 99.7%. After 90 min of treatment, the residual concentration of UO_2^{2+} was reduced to 0.81 ppb, more than 1 order of magnitude lower than the acceptable limit of 30 ppb defined by the US EPA. The kinetic data were fitted with the pseudo-second-order kinetic model, which can be described by the following equation:

$$\frac{t}{q_t} = \frac{1}{k_2 q_e^{\,2}} + \frac{t}{q_e}$$

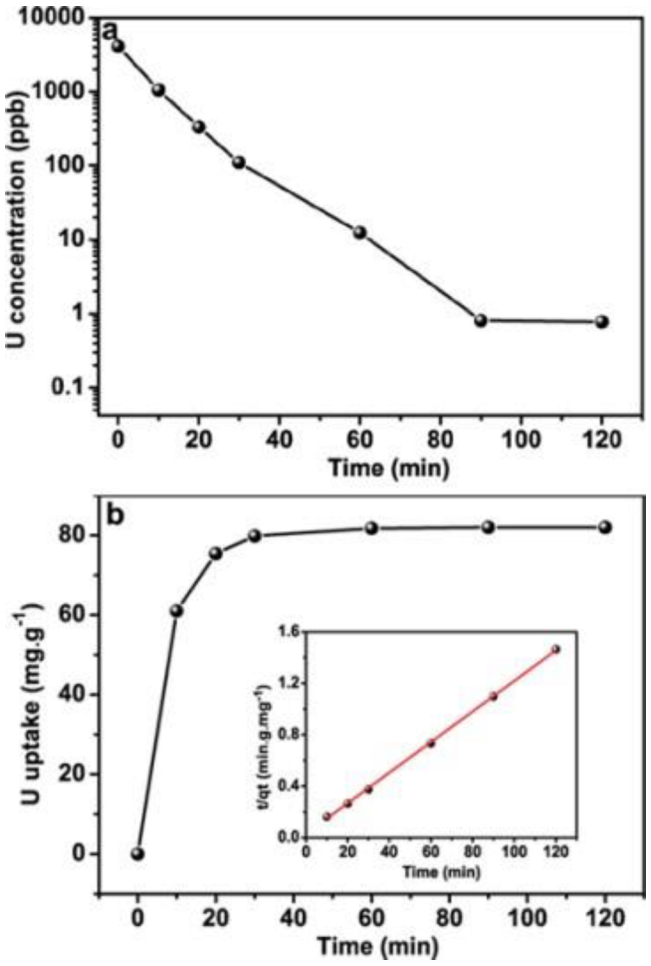

Figure 4. (a) UO_2^{2+} sorption kinetics of PAF-1-CH_2AO under the UO_2^{2+} initial concentration of 4100 ppb with a V/m ratio at 20 000 mL g^{-1}. (b) Adsorption curve of UO_2^{2+} versus contact time in aqueous solution using PAF-1-CH_2AO. Inset shows the pseudo-second-order kinetic plot for the adsorption.

Here, k_2 is the pseudo-second-order rate constant of adsorption (g mg^{-1} min^{-1}). The quantities q_e and q_t are the amount of metal ion adsorbed (mg g^{-1}) at equilibrium and at time t, respectively, and t is adsorption time (min). The plots of t/q_t vs t of the kinetic data showed perfect linear relation (the inset in Figure 4b), yielding a correlation coefficient of R^2 = 0.999 54, which indicates that the rate-limiting step of the adsorption process is chemical adsorption. These results clearly suggest the potential of using PAF-1-CH_2AO for efficient and effective decontamination of wastewater polluted by highly toxic and radioactive uranium.

To further demonstrate the applicability of PAF-1-CH_2AO, the distribution coefficient value (K_d) was calculated using the following equation:

$$K_d = \left(\frac{C_i - C_e}{C_e}\right)\frac{V}{m}$$

where V is the volume of the treated solution (mL), m is the amount of adsorbent (g), C_i is the initial concentration of UO_2^{2+}, and C_e is the equilibrium concentration of UO_2^{2+}. The value of K_d reflects the affinity and selectivity of the sorbents and is an important parameter for a sorbent's performance metrics. A K_d value of 1.0×10^5 mL g^{-1} is generally regarded as excellent. Remarkably, PAF-1-CH_2AO affords an outstanding K_d value of 1.05×10^6 mL g^{-1} (calculated based under the condition of V/m = 20 000 mL g^{-1} with initial UO_2^{2+} concentration of 4100 ppb).

Encouraged by the above results, we tested the performance of PAF-1-CH_2AO in recovery of uranium from simulated seawater to evaluate its potential in the enrichment of uranium from the ocean. We observed PAF-1-CH_2AO is able to adsorb UO_2^{2+} (7.05 ppm) in the presence of a tremendous excess of NaCl and $NaHCO_3$ (25.6 g L^{-1} of NaCl and 0.198 g L^{-1} of $NaHCO_3$, respectively), giving rise to a moderate to high adsorption capacity of about 40 mg g^{-1} (Figure S2), thus suggesting PAF-1-CH_2AO is a promising candidate for recovery of uranium from the ocean.

To gain insight into the coordination environment of uranium in PAF-1-CH_2AO, we employed X-ray absorption fine structure (XAFS) spectroscopy. Data were collected at the uranium L_{III}-edge (17.166 keV) on beamline 10-BM-B of the Advanced Photon Source[56] and processed using the Demeter software suite of the IFEFFIT package based on FEFF 6.[57,58] As shown in Figure 5, a high quality fit (R = 1.37%; χ_ν^2 = 34.5) of the extended XAFS (EXAFS) data was achieved through application of a structure model for uranium bound by 1.4 ± 0.3 amidoxime ligands in an η^2-motif, with the remaining equatorial plane filled with 0.5 ± 0.3 carbonate and 2.1 ± 0.8 coordinating water molecules. Such results are consistent with crystallographic and computationally based investigations regarding uranyl bonding modes,[59] and the EXAFS spectra possess marked similarities with previously reported data for UO_2^{2+} η^2-bound by amidoxime.[60−62] Importantly, the refined coordination number for the amidoxime ligand is greater than 1, revealing cooperative binding occurs between adjacent amidoxime species inside PAF-1-CH_2AO. Such phenomena have been previously reported to afford high uranium uptake and strong binding in MOFs[24] and may constitute a general design principle for the further development of advanced nanostructured adsorbent materials. Additional experimental details regarding XAFS data collection and analysis are available in the Supporting Information.

DOI: 10.1021/acsami.7b01711
ACS Appl. Mater. Interfaces 2017, 9, 12511−12517

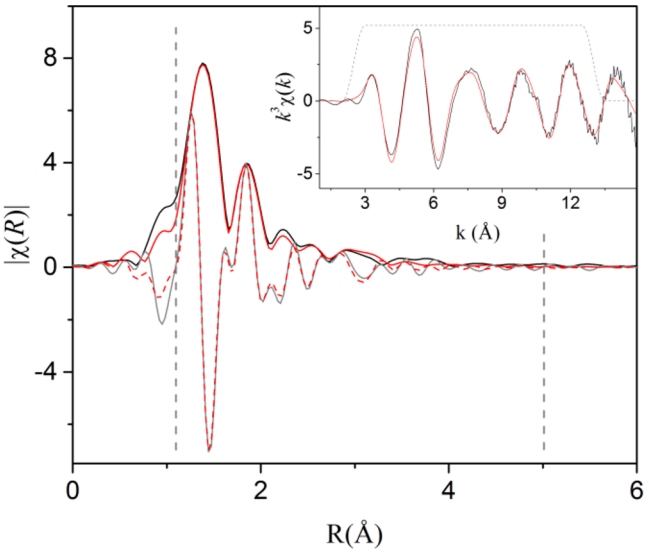

Figure 5. Uranium L_{III}-edge EXAFS spectrum and fit for PAF-1-CH_2AO. Data are k^3-weighted and displayed without phase shift correction. The Fourier transform of the experimental data is in black while the solid red line is the fit. The real component is displayed beneath in gray while the complementary fit is the dashed red line. Inset: the EXAFS data and fit plotted as k^3-weighted $\chi(k)$. In all plots, dashed gray lines depict the fitting region.

CONCLUSION

In summary, we have demonstrated how porous organic polymers can be functionalized for efficient uranium adsorption from water as exemplified by decorating the highly porous and stable POP material, PAF-1, with the uranyl chelating amidoxime group. The resultant amidoxime functionalized PAF-1 (PAF-1-CH_2AO) exhibits excellent uranium extraction performance with a high uranium uptake capacity of over 300 mg g^{-1} and an outstanding distribution coefficient value (K_d) of 1.05×10^6 mL g^{-1} that renders it to effectively reduce the uranyl concentration from 4.1 ppm to less than 1.0 ppb in aqueous solutions, well below the acceptable limit of 30 ppb defined by the US EPA. In addition, PAF-1-CH_2AO is capable of extracting uranium from simulated seawater with a moderately high adsorption capacity of about 40 mg g^{-1}. The local coordination environment of uranium within PAF-1-CH_2AO has also been elucidated by XAFS spectroscopic studies, which suggest the cooperative binding of UO_2^{2+} between adjacent amidoxime species, reasonably interpreting the excellent uranium extraction performances of PAF-1-CH_2AO. Our work not only demonstrates functionalized POPs as a new type of adsorbent material for efficient uranium extraction from aqueous solutions but also provides a task-specific design principle for the development of advanced porous materials for various applications. The design and functionalization of new POPs with enhanced performance in uranium extraction and other contaminants removal are currently underway in our laboratory.

ASSOCIATED CONTENT

Supporting Information

The Supporting Information is available free of charge on the ACS Publications website at DOI: 10.1021/acsami.7b01711.

Characterization details, adsorption kinetics, and XAFS experimental details and analysis (PDF)

AUTHOR INFORMATION

Corresponding Author

*E-mail: sqma@usf.edu (S.M.).

ORCID

Carter W. Abney: 0000-0002-1809-9577

Wenbin Lin: 0000-0001-7035-7759

Shengqian Ma: 0000-0002-1897-7069

Notes

The authors declare no competing financial interest.

ACKNOWLEDGMENTS

This work was supported by the DOE Office of Nuclear Energy's Nuclear Energy University Program (Grant No. DE-NE0008281). Work at the University of Chicago was supported by the U.S. Department of Energy (DOE), Office of Nuclear Energy's Nuclear Energy University Program (Sub-Contract -20 #120427, Project #3151). C.W.A. was supported by the U.S. Department of Energy, Office of Science, Office of Nuclear Energy. This manuscript has been authored by UT-Battelle, LLC under Contract No. DE-AC05-00OR22725 with the U.S. Department of Energy. The United States Government retains and the publisher, by accepting the article for publication, acknowledges that the United States Government retains a nonexclusive, paid-up, irrevocable, worldwide license to publish or reproduce the published form of this manuscript, or allow others to do so, for United States Government purposes. The Department of Energy will provide public access to these results of federally sponsored research in accordance with the DOE Public Access Plan (http://energy.gov/downloads/doe-public-access-plan). MRCAT operations are supported by the Department of Energy and MRCAT member institutions. This research used resources of the Advanced Photon Source, a U.S. Department of Energy (DOE) Office of Science User Facility operated for the DOE Office of Science by Argonne National Laboratory under Contract No. DE-AC02-06CH11357.

REFERENCES

(1) Sholl, D. S.; Lively, R. P. Seven Chemical Separations to Change the World. *Nature* **2016**, *532*, 435−437.

(2) Zhou, L.; Bosscher, M.; Zhang, C.; Özçubukçu, S.; Zhang, L.; Zhang, W.; Li, C. J.; Liu, J.; Jensen, M. P.; Lai, L.; He, C. A Protein Engineered to Bind Uranyl Selectively and with Femtomolar Affinity. *Nat. Chem.* **2014**, *6*, 236−241.

(3) Lu, Y. Coordination Chemistry in the Ocean. *Nat. Chem.* **2014**, *6*, 175−177.

(4) Bardi, U. Extracting Minerals from Seawater: an Energy Analysis. *Sustainability* **2010**, *2*, 980−992.

(5) Macerata, E.; Mossini, E.; Scaravaggi, S.; Mariani, M.; Mele, A.; Panzeri, W.; Boubals, N.; Berthon, L.; Charbonnel, M.-C.; Sansone, F.; Arduini, A.; Casnati, A. Hydrophilic Clicked 2, 6-bis-Triazolyl-Pyridines Endowed with High Actinide Selectivity and Radiochemical Stability: towards a Closed Nuclear Fuel Cycle. *J. Am. Chem. Soc.* **2016**, *138*, 7232−7235.

(6) Yue, Y.; Mayes, R. T.; Kim, J.; Fulvio, P. F.; Sun, X.-G.; Tsouris, C.; Chen, J.; Brown, S.; Dai, S. Seawater Uranium Sorbents: Preparation from a Mesoporous Copolymer Initiator by Atom-Transfer Radical Polymerization. *Angew. Chem., Int. Ed.* **2013**, *52*, 13458−13462.

(7) Sather, A. C.; Berryman, O. B.; Rebek, J., Jr. Selective Recognition and Extraction of the Uranyl Ion from Aqueous Solutions with a Recyclable Chelating Resin. *Chem. Sci.* **2013**, *4*, 3601−3605.

(8) Xie, S.; Liu, X.; Zhang, B.; Ma, H.; Ling, C.; Yu, M.; Li, L.; Li, J. Electrospun Nanofibrous Adsorbents for Uranium Extraction from Seawater. *J. Mater. Chem. A* **2015**, *3*, 2552−2558.

DOI: 10.1021/acsami.7b01711
ACS Appl. Mater. Interfaces 2017, 9, 12511−12517

(9) Sihn, Y. H.; Byun, J.; Patel, H. A.; Lee, W.; Yavuz, C. T. Rapid Extraction of Uranium Ions from Seawater Using Novel Porous Polymeric Adsorbents. *RSC Adv.* **2016**, *6*, 45968−45976.
(10) Pan, H.-B.; Kuo, L.-J.; Wood, J.; Strivens, J.; Gill, G. A.; Janke, C. J.; Wai, C. M. The Uranium from Seawater Program at the Pacific Northwest National Laboratory: Overview of Marine Testing, Adsorbent Characterization, Adsorbent Durability, Adsorbent Toxicity, and Deployment Studies. *RSC Adv.* **2015**, *5*, 100715−100721.
(11) Li, Y.; Wang, L.; Li, B.; Zhang, M.; Wen, R.; Guo, X.; Li, X.; Zhang, J.; Li, S.; Ma, L. Pore-Free Matrix with Cooperative Chelating of Hyperbranched Ligands for High-Performance Separation of Uranium. *ACS Appl. Mater. Interfaces* **2016**, *8*, 28853−28861.
(12) Barber, P. S.; Kelley, S. P.; Griggs, C. S.; Wallace, S.; Rogers, R. D. Surface Modification of Ionic Liquid-spun Chitin Fibers for the Extraction of Uranium from Seawater: Seeking the Strength of Chitin and the Chemical Functionality of Chitosan. *Green Chem.* **2014**, *16*, 1828−1836.
(13) Kou, S.; Yang, Z.; Sun, F. Protein Hydrogel Microbeads for Selective Uranium Mining from Seawater. *ACS Appl. Mater. Interfaces* **2017**, *9*, 2035.
(14) Manos, M. J.; Kanatzidis, M. G. Layered Metal Sulfides Capture Uranium from Seawater. *J. Am. Chem. Soc.* **2012**, *134*, 16441−16446.
(15) Ling, L.; Zhang, W. Enrichment and Encapsulation of Uranium with Iron Nanoparticle. *J. Am. Chem. Soc.* **2015**, *137*, 2788−2791.
(16) Feng, M.-L.; Sarma, D.; Qi, X.-H.; Du, K.-Z.; Huang, X.-Y.; Kanatzidis, M. G. Efficient Removal and Recovery of Uranium by a Layered Organic-Inorganic Hybrid Thiostannate. *J. Am. Chem. Soc.* **2016**, *138*, 12578−12585.
(17) Tripathi, S.; Bose, R.; Roy, A.; Nair, S.; Ravishankar, N. Synthesis of Hollow Nanotubes of Zn_2SiO_4 or SiO_2: Mechanistic Understanding and Uranium Adsorption Behavior. *ACS Appl. Mater. Interfaces* **2015**, *7*, 26430−26436.
(18) Wang, L.; Yuan, L.; Chen, K.; Zhang, Y.; Deng, Q.; Du, S.; Huang, Q.; Zheng, L.; Zhang, J.; Chai, Z.; Barsoum, M. W.; Wang, X.; Shi, W. *ACS Appl. Mater. Interfaces* **2016**, *8*, 16396−16403.
(19) Vivero-Escoto, J. L.; Carboni, M.; Abney, C. W.; deKrafft, K. E.; Lin, W. Organo-Functionalized Mesoporous Silicas for Efficient Uranium Extraction. *Microporous Mesoporous Mater.* **2013**, *180*, 22−31.
(20) Gunathilake, C.; Górka, J.; Dai, S.; Jaroniec, M. Amidoxime-Modified Mesoporous Silica for Uranium Adsorption under Seawater Conditions. *J. Mater. Chem. A* **2015**, *3*, 11650−11659.
(21) Carboni, M.; Abney, C. W.; Taylor-Pashow, K. M. L.; Vivero-Escoto, J. L.; Lin, W. Uranium Sorption with Functionalized Mesoporous Carbon Materials. *Ind. Eng. Chem. Res.* **2013**, *52*, 15187−15197.
(22) Wang, F.; Li, H.; Liu, Q.; Li, Z.; Li, R.; Zhang, H.; Liu, L.; Emelchenko, G. A.; Wang, J. A Graphene Oxide/Amidoxime Hydrogel for Enhanced Uranium Capture. *Sci. Rep.* **2016**, *6*, 19367.
(23) Barber, P. S.; Kelley, S. P.; Rogers, R. D. Highly Selective Extraction of the Uranyl Ion with Hydrophobic Amidoxime-Functionalized Ionic Liquids via η^2 Coordination. *RSC Adv.* **2012**, *2*, 8526−8530.
(24) Carboni, M.; Abney, C. W.; Liu, S.; Lin, W. Highly Porous and Stable Metal-Organic Frameworks for Uranium Extraction. *Chem. Sci.* **2013**, *4*, 2396−2402.
(25) Bai, Z.-Q.; Yuan, L.-Y.; Zhu, L.; Liu, Z.-R.; Chu, S.-Q.; et al. Introduction of Amino Groups into Acid-Resistant MOFs for Enhanced U (VI) Sorption. *J. Mater. Chem. A* **2015**, *3*, 525−534.
(26) Li, L.; Ma, W.; Shen, S.; Huang, H.; Bai, Y.; Liu, H. A Combined Experimental and Theoretical Study on the Extraction of Uranium by Amino-Derived Metal-Organic Frameworks through Post-Synthetic Strategy. *ACS Appl. Mater. Interfaces* **2016**, *8*, 31032−31041.
(27) Kuhn, P.; Antonietti, M.; Thomas, A. Porous, Covalent Triazine-Based Frameworks Prepared by Ionothermal Synthesis. *Angew. Chem., Int. Ed.* **2008**, *47*, 3450−3453.
(28) Cooper, A. I. Conjugated Microporous Polymers. *Adv. Mater.* **2009**, *21*, 1291−1295.
(29) Xu, Y.; Jin, S.; Xu, H.; Nagai, A.; Jiang, D. Conjugated Microporous Polymers: Design, Synthesis and Application. *Chem. Soc. Rev.* **2013**, *42*, 8012−8031.
(30) Makal, T. A.; Li, J.-R.; Lu, W.; Zhou, H.-C. Methane Storage in Advanced Porous Materials. *Chem. Soc. Rev.* **2012**, *41*, 7761−7779.
(31) Yuan, Y.; Sun, F.; Li, L.; Cui, P.; Zhu, G. Porous Aromatic Frameworks with Anion-Templated Pore Apertures Serving as Polymeric Sieves. *Nat. Commun.* **2014**, *5*, 4260.
(32) Qiao, Z.-A.; Chai, S.-H.; Nelson, K.; Bi, Z.; Chen, J.; Mahurin, S. M.; Zhu, X.; Dai, S. Polymeric Molecular Sieve Membranes via in Situ Cross-Linking of Non-Porous Polymer Membrane Templates. *Nat. Commun.* **2014**, *5*, 3705.
(33) Dawson, R.; Adams, D. J.; Cooper, A. I. Chemical Tuning of CO_2 Sorption in Robust Nanoporous Organic Polymers. *Chem. Sci.* **2011**, *2*, 1173−1177.
(34) Liebl, M. R.; Senker, J. Microporous Functionalized Triazine-Based Polyimides with High CO_2 Capture Capacity. *Chem. Mater.* **2013**, *25*, 970−980.
(35) Zhang, Y.; Wei, S.; Liu, F.; Du, Y.; Liu, S.; Ji, Y.; Yokoi, T.; Tatsumi, T.; Xiao, F.-S. Superhydrophobic Nanoporous Polymers as Efficient Adsorbents for Organic Compounds. *Nano Today* **2009**, *4*, 135−142.
(36) Sun, Q.; Aguila, B.; Verma, G.; Liu, X.; Dai, Z.; Deng, F.; Meng, X.; Xiao, F.-S.; Ma, S. Superhydrophobicity: Constructing Homogeneous Catalysts into Superhydrophobic Porous Frameworks to Protect Them from Hydrolytic Degradation. *Chem.* **2016**, *1*, 628−639.
(37) Kaur, P.; Hupp, J. T.; Nguyen, S. T. Porous Organic Polymers in Catalysis: Opportunities and Challenges. *ACS Catal.* **2011**, *1*, 819−835.
(38) Zhang, Y.; Riduan, S. N. Functional Porous Organic Polymers for Heterogeneous Catalysis. *Chem. Soc. Rev.* **2012**, *41*, 2083−2094.
(39) Sun, Q.; Dai, Z.; Meng, X.; Xiao, F.-S. Porous Polymer Catalysts with Hierarchical Structures. *Chem. Soc. Rev.* **2015**, *44*, 6018−6034.
(40) Sun, Q.; Dai, Z.; Meng, X.; Wang, L.; Xiao, F.-S. Task-Specific Design of Porous Polymer Heterogeneous Catalysts beyond Homogeneous Counterparts. *ACS Catal.* **2015**, *5*, 4556−4567.
(41) Sun, Q.; Liu, X.; Sheng, N.; Deng, F.; Meng, X.; Xiao, F.-S. Highly Efficient Heterogeneous Hydroformylation over Rh-Metalated Porous Organic Polymers: Synergistic Effect of High Ligand Concentration and Flexible Framework. *J. Am. Chem. Soc.* **2015**, *137*, 5204−5209.
(42) Banerjee, D.; Elsaidi, S. K.; Aguila, B.; Li, B.; Kim, D.; Schweiger, M. J.; Kruger, A. A.; Doonan, C. J.; Ma, S.; Thallapally, P. Removal of Pertechnetate-Related Oxyanions from Solution Using Functionalized Hierarchical Porous Frameworks. *Chem. - Eur. J.* **2016**, *22*, 17581−17584.
(43) Li, B.; Zhang, Y.; Ma, D.; Shi, Z.; Ma, S. Mercury Nano-Trap for Effective and Efficient Removal of Mercury (II) from Aqueous Solution. *Nat. Commun.* **2014**, *5*, 5537.
(44) Ye, Y.; Zhang, L.; Peng, Q.; Wang, G.; Shen, Y.; Li, Z.; Wang, L.; Ma, X.; Chen, Q.-H.; Zhang, Z.; Xiang, S. High Anhydrous Proton Conductivity of Imidazole-Loaded Mesoporous Polyimides over a Wide Range from Subzero to Moderate Temperature. *J. Am. Chem. Soc.* **2015**, *137*, 913−918.
(45) Zhao, Q.; Heyda, J.; Dzubiella, J.; Täuber, K.; Dunlop, J. W. C.; Yuan, J. Sensing Solvents with Ultrasensitive Porous Poly (ionic liquid) Actuators. *Adv. Mater.* **2015**, *27*, 2913−2917.
(46) Côté, A. P.; Benin, A. I.; Ockwig, N. W.; O'Keeffe, M.; Matzger, A. J.; Yaghi, O. M. Porous, Crystalline, Covalent Organic Frameworks. *Science* **2005**, *310*, 1166−1170.
(47) Feng, X.; Ding, X.; Jiang, D. Covalent Organic Frameworks. *Chem. Soc. Rev.* **2012**, *41*, 6010−6022.
(48) Ding, S.-Y.; Wang, W. Covalent Organic Frameworks (COFs): from Design to Applications. *Chem. Soc. Rev.* **2013**, *42*, 548−568.
(49) Bunck, D. N.; Dichtel, W. R. Internal Functionalization of Three-Dimensional Covalent Organic Frameworks. *Angew. Chem., Int. Ed.* **2012**, *51*, 1885−1889.
(50) Chandra, S.; Kandambeth, S.; Biswal, B. P.; Lukose, B.; Kunjir, S. M.; Chaudhary, M.; Babarao, R.; Heine, T.; Banerjee, R. Chemically

DOI: 10.1021/acsami.7b01711
ACS Appl. Mater. Interfaces 2017, 9, 12511−12517

Stable Multilayered Covalent Organic Nanosheets from Covalent Organic Frameworks via Mechanical Delamination. *J. Am. Chem. Soc.* **2013**, *135*, 17853−17861.
(51) Zhou, H.-C.; Kitagawa, S. Metal-Organic Frameworks (MOFs). *Chem. Soc. Rev.* **2014**, *43*, 5415−5418.
(52) Li, B.; Zhang, Y.; Ma, D.; Xing, Z.; Ma, T.; Shi, Z.; Ji, X.; Ma, S. Creation of a New Type of Ion Exchange Materials for Rapid, High-Capacity, Reversible and Selective Ion Exchange without Swelling and Entrainment. *Chem. Sci.* **2016**, *7*, 2138−2144.
(53) Ben, T.; Ren, H.; Ma, S.; Cao, D.; Lan, J.; Jing, X.; Wang, W.; Xu, J.; Deng, F.; Simmons, J. M.; Qiu, S.; Zhu, G. Targeted Synthesis of a Porous Aromatic Framework with High Stability and Exceptionally High Surface Area. *Angew. Chem., Int. Ed.* **2009**, *48*, 9457−9461.
(54) Yuan, D.; Lu, W.; Zhao, D.; Zhou, H.-C. Highly Stable Porous Polymer Networks with Exceptionally High Gas-Uptake Capacities. *Adv. Mater.* **2011**, *23*, 3723−3725.
(55) Das, S.; Tsouris, C.; Zhang, C.; Kim, J.; Brown, S.; Oyola, Y.; Janke, C. J.; Mayes, R. T.; Kuo, L.-J.; Wood, J. R.; Gill, G. A.; Dai, S. Enhancing Uranium Uptake by Amidoxime Adsorbent in Seawater: An Investigation for Optimum Alkaline Conditioning Parameters. *Ind. Eng. Chem. Res.* **2016**, *55*, 4294−4302.
(56) Kropf, A. J.; Katsoudas, J.; Chattopadhyay, S.; Shibata, T.; Lang, E. A.; Zyryanov, V. N.; Ravel, B.; McIvor, K.; Kemner, K. M.; Scheckel, K. G.; Bare, S. R.; Terry, J.; Kelly, S. D.; Bunker, B. A.; Segre, C. U.; et al. The New MRCAT (Sector 10) Bending Magnet Beamline at the Advanced Photon Source. *AIP Conf. Proc.* **2009**, *1234*, 299−302.
(57) Ravel, B.; Newville, M. Athena, Artemis, Hephaestus: Data Analysis for X-Ray Absorption Spectroscopy Using IFEFFIT. *J. Synchrotron Radiat.* **2005**, *12*, 537−541.
(58) Rehr, J. J.; Albers, R. C. Theoretical Approaches to X-Ray Absorption Fine Structure. *Rev. Mod. Phys.* **2000**, *72*, 621−654.
(59) Vukovic, S.; Watson, L. A.; Kang, S. O.; Custelcean, R.; Hay, B. P. How Amidoximate Binds the Uranyl Cation. *Inorg. Chem.* **2012**, *51*, 3855−3859.
(60) Abney, C. W.; Mayes, R. T.; Piechowicz, M.; Lin, Z.; Bryantsev, V.; Veith, G. M.; Dai, S.; Lin, W. XAFS Investigation of Polyamidoxime-Bound Uranyl Contests the Paradigm from Small Molecule Studies. *Energy Environ. Sci.* **2016**, *9*, 448−453.
(61) Abney, C. W.; Das, S.; Mayes, R. T.; Kuo, L.-J.; Wood, J.; Gill, G.; Piechowicz, M.; Lin, Z.; Lin, W.; Dai, S. A Report on Emergent Uranyl Binding Phenomena by an Amidoxime Phosphonic Acid Co-Polymer. *Phys. Chem. Chem. Phys.* **2016**, *18*, 23462−23468.
(62) Zhang, L.; Su, J.; Yang, S.; Guo, X.; Jia, Y.; Chen, N.; Zhou, J.; Zhang, S.; Wang, S.; Li, J.; Li, J.; Wu, G.; Wang, J.-Q. Extended X-ray Absorption Fine Structure and Density Functional Theory Studies on the Complexation Mechanism of Amidoximate Ligand to Uranyl Carbonate. *Ind. Eng. Chem. Res.* **2016**, *55*, 4224−4230.

NOTE ADDED AFTER ASAP PUBLICATION

This paper was published on the Web on March 31, 2017. UO^{2+} was changed to UO_2^{2+} throughout the document, and the corrected version was reposted on April 12, 2017.

DOI: 10.1021/acsami.7b01711
ACS Appl. Mater. Interfaces 2017, 9, 12511−12517